

Properties of fragmented repulsive condensates

Alexej I. Streltsov and Lorenz S. Cederbaum

Theoretische Chemie, Universität Heidelberg, D-69120 Heidelberg, Germany

(Dated: March 23, 2022)

Abstract

Repulsive Bose-Einstein condensates immersed into a double-well trap potential are studied within the framework of the recently introduced mean-field approach which allows for bosons to reside in several different orthonormal orbitals. In the case of a one-orbital mean-field theory (Gross-Pitaevskii) the ground state of the system reveals a bifurcation scenario at some critical values of the interparticle interaction and/or the number of particles. At about the same values of the parameters the two-orbital mean-field predicts that the system becomes two-fold fragmented. By applying the three-orbital mean field we verify numerically that for the double-well external potential studied here the overall best mean-field is achieved with two orbitals. The variational principle minimizes the energy at a vanishing population of the third orbital. To discuss the energies needed to remove a boson from and the energies gained by adding a boson to the condensate, we introduce boson ionization potentials and boson affinities and relate them to the chemical potentials. The impact of the finite number of bosons in the condensate on these quantities is analyzed. We recall that within the framework of the multi-orbital mean-field theory each fragment is characterized by its own chemical potential. Finally, the stability of fragmented states is discussed in terms of the boson transfer energy which is the energy needed to transfer a boson from one fragment to another.

PACS numbers: 03.75.Hh, 03.65.Ge, 03.75.Nt

I. INTRODUCTION

The experimental realization of Bose-Einstein condensation provides an unique opportunity to study macroscopic quantum systems. One of the key property of a quantum system is the formation of shell structures. For a system of N identical fermions the formation of the shell structure is enforced by the Fermi-statistic, which implies a restriction to the number of particles residing in a single quantum level. In contrast, for bosonic systems where the Bose-statistic permits any occupation numbers, the formation of shell structures, also known as the fragmentation phenomenon [1], must be caused by other reasons.

Fragmentation can appear naturally in condensates made of different kinds of bosons. Binary mixtures of trapped Bose-Einstein condensates have been the subject of numerous experimental [2, 3] and theoretical investigations [4, 5, 6, 7, 8]. These studies comprise binary mixtures made of two different alkalis such as $^{87}\text{Rb} - ^{23}\text{Na}$ [5, 6], of two different isotopes of the same atom $^{87}\text{Rb} - ^{85}\text{Rb}$ [4, 6], and of two different hyperfine states of the same alkali such as the ($F = 2, M_F = 2$) and ($F = 1, M_F = -1$) states of ^{87}Rb [2].

In contrast, the fragmentation phenomenon in BEC made of atoms of one kind and in the same internal state, i.e., made of an identical bosons, is an open theoretical frontier. Traditionally, BEC is described at the Gross-Pitaevskii (GP) mean-field level [9, 10], where all bosons are residing in a single one-particle state. This one-orbital mean-field has been a very successful approximation and can explain many experiments; see, e.g., Refs. [11, 12] and references therein. However, this mean-field intrinsically cannot describe fragmentation. The best mean-field approach allowing for bosons to reside in several different orthonormal orbitals has been formulated recently [13, 14]. Each of the involved orbitals is characterized by a different spatial distribution (localization in space), a different occupation number (number of bosons residing in the orbital), and a different chemical potential. This multi-orbital approach includes the Gross-Pitaevskii theory as a special case, namely when all bosons reside in a single orbital. The multi-orbital mean-field approach is based on a variational principle and hence the optimal orbitals and their occupation numbers are determined variationally such that the energy of the system is minimized. In practice this means that the question whether a BEC forms a fragmented state (shell structure) or prefers to stay in a non-fragmented state (GP) is answered in the framework of one and the same method.

By applying this multi-orbital mean-field to study a repulsive BEC in multi-well ex-

ternal potentials we found [15] that the ground state may be many-fold fragmented, i.e., the macroscopic occupation of several one-particle functions is energetically more favorable than the accumulation of all bosons in a single orbital. The quantities determining the fragmentation are the number of particles, the strength of the interparticle interaction and, of course, the specific shape of the external potential. The influence of all these parameters on fragmentation has been investigated in some detail.

In this paper we consider a system of N identical bosons with positive scattering length immersed into a double-well external potential. The Hamiltonian of this system is defined in Sec.II. In Sec.III we demonstrate that within the standard one-orbital mean-field theory (Gross-Pitaevskii), the ground state of the system reveals a bifurcation scenario starting from a critical value of the interparticle interaction strength or of the number of particles. By applying two-orbital mean-field theory we show in Sec.IV that the ground state of the system made of N identical bosons can indeed be two-fold fragmented. The fragmentation phenomenon starts to take place in the vicinity of the bifurcation point obtained at the GP mean-field level. In Sec.V we apply three-orbital mean-field theory and demonstrate that for the external potential studied here the overall best mean-field is achieved for two orbitals, i.e., the inclusion of a third orbital in the calculation does not improve the mean-field description and the lowest energy is obtained if only two orbitals are occupied.

Sec.VI opens a second part of the present investigation, where we introduce characteristic quantities which allow us to distinguish, at least in principle, between fragmented and non-fragmented states of the condensates. In particular, by comparing the systems of N and $N \pm 1$ bosons we adapt quantities relevant to fermionic systems and define vertical and adiabatic ionization potentials and affinities for bosonic systems. Their relevance to an experimental observation of fragmented states is also addressed. In Sec.VII we introduce a boson transfer energy as the energy needed to transfer a boson from one orbital to another one and use it to analyze the stability of fragmented states. The discussion of the large N -limit of the boson ionization potential, boson affinity and boson transfer energy is presented in Sec.VIII. Finally, Sec.IX summarizes our results and conclusions.

II. THE SYSTEM AND HAMILTONIAN

Our general intention is to consider a system of N identical bosons interacting via a δ -function contact potential $W(\vec{r}_i - \vec{r}_j) = \lambda_0 \delta(\vec{r}_i - \vec{r}_j)$, where \vec{r}_i is the position of the i -th boson and the nonlinear parameter λ_0 is related to the s-wave scattering length of the bosons [12]. The Hamiltonian of this system takes on the standard form

$$\hat{H} = \sum_{i=1}^N \left[-\frac{\hbar^2}{2m} \nabla_{\vec{r}_i}^2 + V(\vec{r}_i) \right] + \sum_{i>j=1}^N W(\vec{r}_i - \vec{r}_j). \quad (1)$$

We denote as $h(\vec{r}) = \hat{T} + V(\vec{r})$ the unperturbed one-particle Hamiltonian consisting of the kinetic operator \hat{T} and the external potential $V(\vec{r})$.

In this work we specifically study bosons trapped in the one-dimensional double-well external potential shown in the insets of Fig.1. Effectively the trap is obtained as an "inner" potential

$$V_{inner}(x) = \omega \left(\frac{x^2}{2} - 0.8 \right) e^{-0.02(x^2 + 0.25x^3 + 6.1x)} \quad (2)$$

and an "outer" trap V_{outer} which consists of an infinite wall at $x = 9.5\pi$ where the inner potential has already died off. The resulting combined potential ($V(x) = V_{inner} + V_{outer}$) has two well-separated nonequivalent wells. It should be mentioned that the results discussed here hardly depend on whether the infinite wall of V_{outer} is replaced by a smoothly growing potential wall [15]. The kinetic energy reads $\hat{T} = -\frac{\omega}{2} \frac{\partial^2}{\partial x^2}$ implying that the coordinate x is dimensionless while all energies and λ_0 are now in units of the frequency ω .

We would like to stress that all conclusions and qualitative results discussed in this work also apply to other double-well external potentials like, for instance, that used in the experimental set up of Ref.[16].

III. GROSS-PITAEVSKII MEAN-FIELD RESULTS

The standard one-orbital mean-field description of the interacting system is obtained by assuming that the ground state wave function Ψ is a product of identical spatial orbitals φ : $\Psi(\vec{r}_1, \vec{r}_2, \dots, \vec{r}_N) = \varphi(\vec{r}_1)\varphi(\vec{r}_2) \cdots \varphi(\vec{r}_N)$. The energy $E \equiv \langle \Psi | \hat{H} | \Psi \rangle$, defined as the expectation value of the \hat{H} , reads

$$E_{GP} = N \left\{ \int \varphi^* h \varphi d\vec{r} + \frac{\lambda}{2} \int |\varphi|^4 d\vec{r} \right\}, \quad (3)$$

where $\lambda = \lambda_0(N-1)$ is the interaction parameter. By minimizing this energy the well-known Gross-Pitaevskii equation [9, 10] is obtained

$$\{h(\vec{r}) + \lambda_0(N-1)|\varphi(\vec{r})|^2\}\varphi(\vec{r}) = \mu_{GP}\varphi(\vec{r}). \quad (4)$$

The only parameter involved in the Gross-Pitaevskii mean-field is $\lambda = \lambda_0(N-1)$. Therefore, all systems which are characterized by the same λ have the same energy per particle as well as the same orbital $\varphi(\vec{r})$ even if the systems have different numbers of bosons. Below, we will use this fact to compare systems made of different numbers of bosons but have the same value of λ .

We solved the Gross-Pitaevskii equation with the external potential introduced in Sec. II for different values of λ . In Fig. 1 we plot the energy per particle of the lowest energy solutions as a function of λ . From this figure it can be inferred that the energy per particle of the ground state increases monotonically with λ up to some critical value of $\lambda_{cr} = 0.837$ and then the energy trajectory is split into two branches. This critical value of λ is indicated in Fig. 1 by a vertical dashed line. The single-particle wavefunction (orbital) corresponding to the upper branch, marked as I in Fig. 1, is depicted in the upper inset of Fig. 1. This wavefunction is mainly localized in the left well. From λ_{cr} on, the lowest energy branch, labeled II in Fig. 1, smoothly bifurcates from the "localized" solution and describes a delocalization of the BEC over the two wells. This delocalized solution is depicted in the right bottom inset of Fig. 1. For convenience, we also plot in both insets the rescaled double-well potential $V/10$. The bifurcation scenario is a known feature [17, 18, 19, 20, 21, 22] of the Gross-Pitaevskii equation reflecting the non-linearity of the underlying mean-field approximation. Bifurcations have been predicted for the ground [17, 18, 20, 21, 22] and excited [18, 19, 21] states of repulsive [18, 19, 20, 21] and attractive [17, 18, 20, 21, 22] condensates confined in different trap potentials.

Within the Gross-Pitaevskii mean field we obtain the following physical picture of Bose-Einstein condensation of repulsive bosons immersed into non-symmetric double-well potentials. For $\lambda < \lambda_{cr}$ the BEC is localized in the deeper well only. When λ is increased, the BEC may continue to be localized in this well, but it is energetically more favorable for bosons to tunnel through the barrier and to populate also the other well. As we have mentioned above, $\lambda = \lambda_0(N-1)$ is the only relevant parameter, and therefore both localization and delocalization phenomena can be observed for systems made of any number of particles by

properly tuning the interparticle interaction strength λ_0 .

IV. TWO-ORBITAL MEAN-FIELD RESULTS

In the previous section we demonstrated that above some critical value of nonlinearity λ_{cr} the ground state of the system is described in the GP approach by a wave function delocalized over both wells. The existence of a bifurcation in the GP results can be seen as a hint to go beyond the GP theory. The natural question arises whether it is possible to improve the GP mean-field description by providing a more flexible mean-field ansatz which would allow bosons to occupy two different orbitals which, in principle, could be localized in different wells.

Recently, a multi-orbital mean-field approach allowing for bosons to reside in several different orthonormal one-particle functions has been formulated [13, 14]. Using m different orbitals, the approach is denoted MF(m). In this section we discuss MF(2). In the next section we shall see that for the double-well geometry of the external potential studied here, the overall best mean-field is achieved within the two-orbital mean-field theory. Since the details of the derivations have already been published elsewhere [13, 14], we present here only the final formulae. Assuming that n_1 bosons occupy the orbital ϕ_1 and n_2 bosons occupy the orbital ϕ_2 leads to the following many-body wave function

$$\Psi(\vec{r}_1, \dots, \vec{r}_N) = \hat{\mathcal{S}}\phi_1(\vec{r}_1) \cdots \phi_1(\vec{r}_{n_1})\phi_2(\vec{r}_{n_1+1}) \cdots \phi_2(\vec{r}_{n_1+n_2}), \quad (5)$$

where $\hat{\mathcal{S}}$ is the symmetrizing operator. The MF(2) energy expression takes on the form

$$E = n_1 h_{11} + \lambda_0 \frac{n_1(n_1 - 1)}{2} \int |\phi_1|^4 d\vec{r} + n_2 h_{22} + \lambda_0 \frac{n_2(n_2 - 1)}{2} \int |\phi_2|^4 d\vec{r} + 2\lambda_0 n_1 n_2 \int |\phi_1|^2 |\phi_2|^2 d\vec{r} \quad (6)$$

The optimal orbitals ϕ_1 and ϕ_2 which minimize this energy functional are determined by solving the two coupled non-linear equations:

$$\begin{aligned} \{ h(\vec{r}) + \lambda_0(n_1 - 1)|\phi_1(\vec{r})|^2 + 2\lambda_0 n_2 |\phi_2(\vec{r})|^2 \} \phi_1(\vec{r}) &= \\ &= \mu_{11} \phi_1(\vec{r}) + \mu_{12} \phi_2(\vec{r}) \\ \{ h(\vec{r}) + \lambda_0(n_2 - 1)|\phi_2(\vec{r})|^2 + 2\lambda_0 n_1 |\phi_1(\vec{r})|^2 \} \phi_2(\vec{r}) &= \\ &= \mu_{21} \phi_1(\vec{r}) + \mu_{22} \phi_2(\vec{r}) \end{aligned} \quad (7)$$

Obviously, the GP equations (3) and (4) follow immediately from the MF(2) equations (6) and (7) by putting the occupation of one of the two orbitals to zero.

In contrast to the one-orbital mean-field (GP) description where $\lambda = \lambda_0(N-1)$ is the only parameter involved, the two-orbital mean-field (MF(2)) depends on two parameters n_1 and n_2 which are the occupation numbers of the one-particle orbitals ϕ_1 and ϕ_2 respectively. At fixed interaction strength λ_0 and number of bosons N , the MF energy (see Eq.6) depends on the particular value of n_1 ($n_2 = N - n_1$). It should be noted that the occupation numbers are variational parameters. In order to find their optimal value and that of the energy, Eqs.(7) are solved for all possible occupation numbers, and the corresponding energies are evaluated by using Eq.(6). At the optimal values of the occupation numbers the energy E takes on its minimum and the MF(2) becomes the best two-orbital mean field which we denote by BMF(2).

We solved the MF(2) equations for $\lambda = 0.8$ and for $\lambda = 0.9$. These values of the non-linear parameter have been chosen to be smaller and larger than $\lambda_{cr} = 0.837$ which is the bifurcation point of the GP energy trajectory discussed in Sec.III. In Fig.2 and Fig.3 we plot the MF(2) energies per particle for $\lambda = 0.8$ and for $\lambda = 0.9$, respectively, as a function of the relative occupation number n_1/N of the orbital localized in the deeper (left) well of the trap potential. The results are shown for $N = 5, 10, 25, 10^2, 10^3$ and 10^6 bosons. The GP energy is indicated by the horizontal line and labeled as "GP".

The common feature seen in Figs.2 and 3 is that the energies per particle of the systems of bosons which are characterized by the same $\lambda = \lambda_0(N-1)$ do depend on the number of bosons N and reveal a different dependence on n_1/N . In contrast to the GP approach, the multi-orbital mean-field theory distinguishes between systems with different number of bosons even if they are characterized by the same value of λ . As seen in the figures, for $n_1/N = 1$, i.e., when all bosons reside in one orbital, the energies of all the curves coincide at the same value which is nothing but the corresponding GP energy. We can obviously conclude that the GP approach is indeed a special case of the MF(2) theory.

In Fig.2 and in particular in Fig.3 it is seen that the optimal BMF(2) energies may be lower than the corresponding GP one and in these cases BMF(2) constitutes the proper ground state of the system. These ground states with nonzero occupation numbers are *fragmented* states, because the respective one-particle density matrix has several nonzero eigenvalues [1, 15, 23]. Therefore, the fragmentation observed before in three-well potentials

[15] also persists in double-well external potentials. It is worthwhile to stress that at the minimum of the energy one of the corresponding optimal orbitals is localized in the left well and the other one in the right well of the trap potential. This is in an agreement with the three-fold fragmentation studied before, where the optimal orbitals have also been found to be localized in the different wells of the three-well external potential [15].

Figs.2 and 3 exhibit several interesting features. Let us first discuss Fig.2 where $\lambda = 0.8$ is smaller than λ_{cr} . Inspection of the inset shows that the MF(2) energy curves as a function of n_1/N posses a minimum for $N \leq 14$ bosons. At these minima the energy is below the GP energy which is at the maxima of the curves. For the systems which contain more than 14 particles, the MF(2) energy curves are monotonously increasing and their lowest energy is at the GP energy.

The situation changes drastically for $\lambda = 0.9$ which is larger than λ_{cr} . As seen in the inset of Fig.3, the BMF(2) energy is lower than the GP energy for condensates with up to $N_{max} \approx 102000$ bosons. For all these systems the fragmentation of the ground state is evident and macroscopic. One should be aware that λ is kept fixed in Fig.3 and, therefore, the interparticle interaction strength λ_0 is small for the many-particle systems shown there.

Finally, we would like to point out two additional features of Fig.3. First, the GP energy is a local minimum for most of the energy curves and consequently there appears a maximum which separates this energy from the global minimum, i.e., from the BMF(2) energy. This may hint to an interesting dynamics of fragmentation if the system is initially prepared in a non-fragmented state. Second, although there exists a maximal number of particles, N_{max} , for which the ground state is fragmented, it should be stressed that for *all* $N > N_{max}$ the energy gap between the BMF(2) and GP energies is extremely small. For $N = 10^6$ bosons, for instance, this energy difference per particle is only $\approx 3 \times 10^{-7}$ units of ω . The coexistence of the fragmented and non-fragmented, but delocalized states is of great interest by itself and might play a role in particular in time-dependent experiments.

V. PROOF THAT BMF(2) IS THE BEST OVERALL MEAN FIELD

From the previous section we learned that by allowing bosons to reside in two orbitals, the mean-field description of the repulsive BEC in the double-well potential has improved compared to the standard one-orbital description. The natural question arises whether the

inclusion of even more orbitals can provide further improvement of the mean-field description of the BEC. To answer this question we apply the three-orbital mean-field theory (MF(3)) [15].

The corresponding ansatz for the wavefunction assumes that three orbitals ϕ_1 , ϕ_2 and ϕ_3 are now occupied by n_1, n_2 and $n_3 = N - n_1 - n_2$ bosons, respectively

$$\Psi(\vec{r}_1, \dots, \vec{r}_N) = \hat{\mathcal{S}} \phi_1(\vec{r}_1) \cdots \phi_1(\vec{r}_{n_1}) \phi_2(\vec{r}_{n_1+1}) \cdots \phi_2(\vec{r}_{n_1+n_2}) \phi_3(\vec{r}_{n_1+n_2+1}) \cdots \phi_3(\vec{r}_{n_1+n_2+n_3}), \quad (8)$$

where $\hat{\mathcal{S}}$ is the symmetrizing operator. The three-orbital mean-field energy reads [15]:

$$\begin{aligned} E = n_1 h_{11} + \lambda_0 \frac{n_1(n_1-1)}{2} \int |\phi_1|^4 d\vec{r} + n_2 h_{22} + \lambda_0 \frac{n_2(n_2-1)}{2} \int |\phi_2|^4 d\vec{r} + \\ n_3 h_{33} + \lambda_0 \frac{n_3(n_3-1)}{2} \int |\phi_3|^4 d\vec{r} + 2\lambda_0 n_1 n_2 \int |\phi_1|^2 |\phi_2|^2 d\vec{r} + \\ + 2\lambda_0 n_1 n_3 \int |\phi_1|^2 |\phi_3|^2 d\vec{r} + 2\lambda_0 n_2 n_3 \int |\phi_2|^2 |\phi_3|^2 d\vec{r}. \end{aligned} \quad (9)$$

The optimal orbitals minimizing this energy functional are obtained by solving the following system of three coupled non-eigenvalue equations [15]

$$\begin{aligned} \{ h(\vec{r}) + \lambda_0(n_1-1)|\phi_1(\vec{r})|^2 + 2\lambda_0 n_2 |\phi_2(\vec{r})|^2 + 2\lambda_0 n_3 |\phi_3(\vec{r})|^2 \} \phi_1(\vec{r}) = \\ = \mu_{11} \phi_1(\vec{r}) + \mu_{12} \phi_2(\vec{r}) + \mu_{13} \phi_3(\vec{r}) \\ \{ h(\vec{r}) + \lambda_0(n_2-1)|\phi_2(\vec{r})|^2 + 2\lambda_0 n_1 |\phi_1(\vec{r})|^2 + 2\lambda_0 n_3 |\phi_3(\vec{r})|^2 \} \phi_2(\vec{r}) = \\ = \mu_{21} \phi_1(\vec{r}) + \mu_{22} \phi_2(\vec{r}) + \mu_{23} \phi_3(\vec{r}) \\ \{ h(\vec{r}) + \lambda_0(n_3-1)|\phi_3(\vec{r})|^2 + 2\lambda_0 n_1 |\phi_1(\vec{r})|^2 + 2\lambda_0 n_2 |\phi_2(\vec{r})|^2 \} \phi_3(\vec{r}) = \\ = \mu_{31} \phi_1(\vec{r}) + \mu_{32} \phi_2(\vec{r}) + \mu_{33} \phi_3(\vec{r}). \end{aligned} \quad (10)$$

For the numerical procedure to solve this system of equations and to obtain the self-consistent orbitals ϕ_i and the corresponding values of the Lagrange parameters μ_{ij} ($i, j = 1, 2, 3$), we refer to Ref.[15].

In comparison with the MF(2) approach the MF(3) method has one more variational parameter n_3 . We solved the above system of three coupled equations (10) for several values of λ and N and different fixed values of n_3 . As an example, we show in Fig.4 the results obtained for $\lambda = 0.9$ and $N = 1000$ for different occupation patterns. Keeping the value of the third occupation number n_3/N fixed at 0.0001, 0.001, 0.005 and also at zero, we plot the three-orbital mean-field energy per particle as a function of the relative occupation number

n_1/N . The occupation of the second orbital $n_2 = N - n_1 - n_3$ is, of course, determined by n_1 and n_3 . The three-orbital mean-field method obviously includes MF(2) as a special case, namely, when the occupation of the third orbital vanishes. We see from Fig.4 that increasing the value of n_3/N leads to a gradual increase of the MF(3) energy per particle. Clearly, in the present case of repulsive condensates in the double-well potential, the overall best mean-field is obtained within the two-orbital BMF(2) theory. The enforced inclusion of more orbitals only enhances the energy of the condensate.

Several consequences should be mentioned. First, fragmentation is a general physical phenomenon which takes place in repulsive BECs trapped in multi-well external potentials. Second, the number of the fragments and their occupation numbers are defined variationally, by minimizing the total energy functionals in Eqs.(6) and (9). If more orbitals are included in the mean-field ansatz than needed, the occupation of the superfluous orbitals becomes zero.

VI. SOME PROPERTIES OF FRAGMENTED STATES

Usually, to distinguish fragmented and non-fragmented states a phase difference between wave functions of the different fragments is considered [24, 25, 26]. Dynamical stability [27, 28] of the relative phase between the condensates localized in the different wells and related questions on the evolution of the fragmented state [29, 30] have been a subject of several discussions.

In contrast to these time-dependent studies on fragmentation, we concentrate in the second part of our work on time-independent properties of the stationary fragmented states themselves. The analogy between shell structures (atoms and molecules) formed in the fermionic world and the bosonic fragmented states studied in the previous sections motivates us to make use of some fermionic observables such as the ionization potential and electron affinity, and introduce related quantities for bosonic systems. Indeed, at the multi-orbital mean-field level of description the fermionic system is described by antisymmetrized single-determinant wave function [31], while the symmetrized ansatz (see Eqs.(5) and (8)) is proposed for bosonic systems. The variationally optimal orbitals and the corresponding orbital energies are obtained by solving the well-known Hartree-Fock (HF) equations [31] for fermions and the BMF equations for bosons. The total energies of these systems are

evaluated by computing the expectation values of the full many-body Hamiltonians with the (anti)symmetrized ansatz of the wave function.

The electron ionization potential (IP) is defined as the difference in total energies between the reference system with N electrons and the ionized system with $N - 1$ electrons [31]. Because of this definition, the ionization potential is also referred to as the binding energy of an electron in the system. We define the *boson ionization potential* or the binding energy of a boson as the energy needed to remove a boson from a bosonic system with N bosons. Another very important physical characteristic is the electron affinity defined as the energy gained by adding one electron to the atom or molecule [31]. In analogy, we define the *boson affinity* as the energy gained by attaching one boson to the bosonic system under consideration.

The boson ionization potentials and affinities can be calculated straightforwardly based on their definitions as differences between total energies. In principle, these total energies may be evaluated within the framework of any suitable N-body method, but in the present study we restrict ourselves for consistency to the two-orbital mean-field approach. To distinguish between the total energies of the condensates made of a different number of bosons we introduce superscript indices. In this notation the MF(2) total energies of the system with $N-1$, N and $N+1$ bosons take on the following form $^{N-1}E(n_1, n_2)$, $^NE(n_1, n_2)$, $^{N+1}E(n_1, n_2)$, where the superscript refers to the condensates made of the corresponding number of bosons. We recall that within the framework of the MF(2) approach the total energy of the system is a function of the occupation number n_1 ($n_2 = N - n_1$) and the minimum of this energy is called the best mean field (BMF(2)). Obviously, the MF(2) energies of the systems with a different number of bosons achieve their minimal values (BMF(2) energies) at different values of the occupation numbers. We denote these BMF(2) energies and corresponding occupation numbers as KE_0 and (n_1^K, n_2^K) where the superscript K refers to the system with K bosons.

A. Adiabatic and Vertical boson ionization potentials

The general definition of the boson ionization potential involves the total energies of condensates made of N and $N - 1$ bosons. Usually, the reference system with N bosons is considered to be in its ground equilibrium state while the ionized system with $N - 1$ bosons

can be either in an equilibrium or in a some transitional state. In the following section we verify that only the BMF(2) energy (the minimum of the MF(2) energy curve) corresponds to the equilibrium state of the condensate, while all other MF(2) energies can be attributed to some transitional (non-equilibrium) states of the condensate.

The difference between the ground *equilibrium* state energies of the ionized system with $N - 1$ bosons and the reference system with N bosons is called *adiabatic boson ionization potential* (BIP_A):

$$BIP_A = {}^{N-1}E_0 - {}^NE_0. \quad (11)$$

The equilibrium in the ionized state might be achieved by adiabatically removing a boson from the condensate.

In contrast, if a boson is suddenly removed from the system, then the state created is not an equilibrium state of the ionized system and the difference between the energy of this non-equilibrium state and that of the ground state of the reference system is called *vertical boson ionization potential* (BIP_V). If the bosonic system under consideration is fragmented, then the sudden ionization of a boson from different orbitals of the fragmented state requires different energies. The two-fold fragmented states are characterized by two different vertical boson ionization potentials

$$\begin{aligned} BIP_V(1) &= {}^{N-1}E(n_1^N - 1, n_2^N) - {}^NE_0(n_1^N, n_2^N) \\ BIP_V(2) &= {}^{N-1}E(n_1^N, n_2^N - 1) - {}^NE_0(n_1^N, n_2^N), \end{aligned} \quad (12)$$

where ${}^NE_0 = {}^NE_0(n_1^N, n_2^N)$ is the BMF(2) energy of the reference system with N bosons obtained at the optimal occupation numbers n_1^N and n_2^N of the two fragments and, ${}^{N-1}E(n_1^N - 1, n_2^N)$ and ${}^{N-1}E(n_1^N, n_2^N - 1)$ are the MF(2) energies of the ionized states where a boson has been removed from the first and second fragment, respectively.

In Fig.5A we present a schematic diagram of the adiabatic and vertical ionization potentials together with the MF(2) total energies of the systems with $N + 1$, N and $N - 1$ bosons plotted as functions of the number n_1 of bosons residing in the first orbital. In Fig.5B we plot these quantities as functions of the complementary parameter $n_2 = N - n_1$ (the number of bosons residing in the second orbital). The BMF(2) energies of the systems with $N + 1$, N and $N - 1$ bosons are indicated on the energy axis. The optimal occupation numbers n_1^N

and n_2^N corresponding to the minimum of the MF(2) energy of the reference N-boson system are indicated on the x-axes of Fig.5A and Fig.5B, respectively.

The difference between the ground state energy of the ionized system $^{N-1}E_0$ and that of the reference system NE_0 , i.e., the adiabatic ionization potential, is marked in Fig.5A as BIP_A . The vertical boson ionization potential $BIP_V(2)$ is shown in Fig.5A as a *vertical* line connecting the minimum of the N -particle energy curve and the energy curve of the system with $N - 1$ bosons. Let us explain this construction. When a boson is suddenly removed from the second orbital ϕ_2 of the reference system, the occupation number n_1^N of the other (first) orbital remains the same also in the ionized system, while the occupation of the second orbital in the ionized state is obviously reduced by one to $n_2^N - 1$. Therefore, this ionization process is indicated by the vertical line in the (E, n_1) -diagram.

The vertical boson ionization potential $BIP_V(1)$ is also shown as a vertical line connecting the minimum of the N -particle energy curve and the energy curve of the system with $N - 1$ bosons, but in the complementary $(E, n_2 = N - n_1)$ -diagram (see Fig.5B). In this case the occupation number of the first orbital is reduced by one to $n_1^N - 1$ in the ionized state, while the occupation number of the second orbital n_2^N remains the same as in the reference state. For completeness, the $BIP_V(1)$ and $BIP_V(2)$ are plotted in both panels of figure 5.

Removing a single boson from the system will not cause a strong change of the orbitals of the other bosons and these orbitals can be assumed fixed. In fermionic systems this assumption is known as the *frozen orbital approximation* [31]. This observation allows us to evaluate *approximately* the vertical ionization potentials and hence, the total energies of the ionized systems.

In the frozen orbital approximation we assume that the orbitals of the reference N-bosonic system ϕ_1 and ϕ_2 do not change upon the sudden removal of a boson, i.e., the ionized system is described by the same orbitals as well. The energies of the corresponding ionized states where the boson has been suddenly removed from the ϕ_1 or the ϕ_2 orbital take on the form

$${}^{N-1}E(n_1 - 1, n_2) = (n_1 - 1)h_{11} + \lambda_0 \frac{(n_1 - 1)(n_1 - 2)}{2} \int |\phi_1|^4 d\vec{r} +$$

$$n_2 h_{22} + \lambda_0 \frac{n_2(n_2 - 1)}{2} \int |\phi_2|^4 d\vec{r} + 2\lambda_0(n_1 - 1)n_2 \int |\phi_1|^2 |\phi_2|^2 d\vec{r} \quad (13a)$$

$${}^{N-1}E(n_1, n_2 - 1) = (n_2 - 1)h_{22} + \lambda_0 \frac{(n_2 - 1)(n_2 - 2)}{2} \int |\phi_2|^4 d\vec{r} +$$

$$n_1 h_{11} + \lambda_0 \frac{n_1(n_1 - 1)}{2} \int |\phi_1|^4 d\vec{r} + 2\lambda_0 n_1(n_2 - 1) \int |\phi_1|^2 |\phi_2|^2 d\vec{r} \quad (13b)$$

respectively.

According to the definitions in Eqs.12, the vertical ionization potentials are obtained by substructing the BMF energy ${}^N E_0$ of the reference N-particle state from the energies of the ionized states in Eqs.13a,13b at $n_2 = n_2^N$. We easily find for the boson vertical ionization potentials in the frozen orbital approximation the appealing relations

$$BIP_V(1) = -\mu_{11}$$

$$BIP_V(2) = -\mu_{22}, \quad (14)$$

i.e., they are given by the negative of the respective Lagrange multipliers which we call chemical potentials.

It is worthwhile to recall that at the level of the standard GP theory (see Sec.III) the energy needed to remove a boson from the non-fragmented N-boson condensate without changing the corresponding orbital φ is given by the GP chemical potential:

$${}^{N-1}E_{GP} - {}^N E_{GP} = -\mu_{GP}. \quad (15)$$

The relations between orbital energies and ionization potentials in the fermionic case are the subject of the well-known Koopmans' theorem [31, 32]. Whithin the Hartree-Fock mean field this theorem states that the vertical ionization potential is the negative of the energy of the orbital from which the electron has been removed. Attributing the diagonal Lagrange multipliers (chemical potentials) μ_{ii} to the orbital energies of the fragmented state, the formal results for fermionic and bosonic systems are absolutely identical.

We conclude that the process of sudden ionization of a boson from the non-fragmented GP state is characterized by a single ionization potential while different ionization potentials

characterize a two-fold fragmented state of the condensate. We recall that in the thermodynamic limit the change in the energy of a system obtained by removing a particle is called *chemical potential*. The condensates studied here are made of identical bosons, and, therefore, a single chemical potential is expected to characterize these condensates at equilibrium. This seems to contradict the results obtained here for the two-fold fragmented states, where two, in general different, chemical potentials exist. This apparent contradiction is resolved by remembering that the present results are for finite systems. Indeed, we demonstrate in Sec.VIII that in the limit of a large number of particles these different chemical potentials become identical at the optimal occupations restoring thereby the thermodynamic picture of a condensate.

B. Adiabatic and vertical boson affinities.

The main propose of the present section is to consider a process where a boson is added to the reference system of N bosons. We define *adiabatic boson affinity* (BA_A) as the difference between the ground *equilibrium* state energies of this reference system and of the system which results by attaching a boson to the reference system

$$BA_A = {}^N E_0 - {}^{N+1} E_0. \quad (16)$$

The adiabatic boson affinity is shown schematically in Fig.5A. It describes the energy gained by the attachment of a boson.

Similarly to the sudden ionization process used to introduce the vertical ionization potentials in the previous subsection, we consider the sudden attachment of a boson to the two-fold fragmented state and define two *vertical boson affinities* comprising the sudden attachment of a boson to the ϕ_1 and ϕ_2 fragments, respectively:

$$\begin{aligned} BA_V(1) &= {}^N E_0(n_1^N, n_2^N) - {}^{N+1} E(n_1^N + 1, n_2^N) \\ BA_V(2) &= {}^N E_0(n_1^N, n_2^N) - {}^{N+1} E(n_1^N, n_2^N + 1). \end{aligned} \quad (17)$$

Here, ${}^N E_0 = {}^N E_0(n_1^N, n_2^N)$ is the BMF(2) energy of the reference system, n_1^N and n_2^N are the corresponding optimal occupation numbers, ${}^{N+1} E(n_1^N + 1, n_2^N)$ and ${}^{N+1} E(n_1^N, n_2^N + 1)$ are the MF(2) energies of the states where a boson has been attached to the first and to the

second fragment, respectively. In Fig.5A and Fig.5B we schematically plot the vertical boson affinities $BA_V(2)$ and $BA_V(1)$ as the vertical lines connecting the corresponding points on the energy curves.

In the frozen orbital approximation the energies of the states to which the boson has been suddenly attached to the ϕ_1 or ϕ_2 orbital take on the form

$$\begin{aligned} {}^{N+1}E(n_1 + 1, n_2) = & (n_1 + 1)h_{11} + \lambda_0 \frac{(n_1 + 1)(n_1 - 0)}{2} \int |\phi_1|^4 d\vec{r} + \\ & n_2 h_{22} + \lambda_0 \frac{n_2(n_2 - 1)}{2} \int |\phi_2|^4 d\vec{r} + 2\lambda_0(n_1 + 1)n_2 \int |\phi_1|^2 |\phi_2|^2 d\vec{r} \end{aligned} \quad (18a)$$

$$\begin{aligned} {}^{N+1}E(n_1, n_2 + 1) = & (n_2 + 1)h_{22} + \lambda_0 \frac{(n_2 + 1)(n_2 - 0)}{2} \int |\phi_2|^4 d\vec{r} + \\ & n_1 h_{11} + \lambda_0 \frac{n_1(n_1 - 1)}{2} \int |\phi_1|^4 d\vec{r} + 2\lambda_0 n_1(n_2 + 1) \int |\phi_1|^2 |\phi_2|^2 d\vec{r} \end{aligned} \quad (18b)$$

By subtracting these energies from the BMF energy of the reference N-particle state ${}^N E_0$, we obtain the vertical boson affinities $BA_V(1)$ and $BA_V(2)$ in the frozen orbital approximation:

$$\begin{aligned} BA_V(1) = & -\mu_{11} - \lambda_0 \int |\phi_1|^4 d\vec{r} \\ BA_V(2) = & -\mu_{22} - \lambda_0 \int |\phi_2|^4 d\vec{r}. \end{aligned} \quad (19)$$

Interestingly, the vertical boson affinities in the frozen orbital approximation are not fully determined by the chemical potentials in contrast to our finding for the vertical boson ionization potentials discussed in the preceding subsection.

It is informative to notice that the energy gained by adding a boson to the non-fragmented condensate without changing the corresponding orbital φ for a finite number of bosons reads:

$${}^N E_{GP} - {}^{N+1} E_{GP} = -\mu_{GP} - \lambda_0 \int |\varphi|^4 d\vec{r}. \quad (20)$$

Hence, even at the level of the standard GP theory, the energy needed to remove a boson from a non-fragmented condensate differs from that gained by adding a boson to this condensate.

The above findings reveal differences between bosonic and fermionic systems. In contrast to the electron affinity which in the framework of the Hartree-Fock mean-field approach is given by the negative of the virtual orbital's energy, the boson affinity does not depend on the virtual orbital and, in addition, is subject to a correction term proportional to λ_0 .

C. Numerical examples

For illustration purposes we evaluate all the above introduced adiabatic and vertical boson ionization potentials and boson affinities for several reference systems made of $N = 5, 10, 25, 100$ and 1000 bosons, keeping $\lambda = 0.9$ fixed throughout. In the GP theory all these systems are characterized by the same chemical potential. Tab.I summarizes the computational results on the vertical boson ionization potentials and vertical boson affinities obtained within the framework of the direct scheme in Eqs.12 and 17, respectively. For comparison we also evaluate all these quantities using the frozen orbital approximation as given in Eqs.14 and 19. In Tab.I these approximate numbers are given in parenthesis. By comparing all these quantities we conclude that the frozen orbital approximation provides very accurate results for the systems with a large number of bosons and surprisingly accurate results for the system with a small number of bosons.

The main physical conclusion derived is that the two-fold fragmented states are characterized by two different vertical ionization potentials and by two different vertical boson affinities. In contrast, the non-fragmented GP state is characterized by a single ionization potential and single affinity. At least in principle, this difference might be used to distinguish fragmented and non-fragmented states. The values of the various vertical boson ionization potentials and vertical boson affinities differ from each other clearly for the systems made of a small number of bosons. As the number of bosons increases, all these values become more similar to each other and also to the negative of the GP chemical potential.

Closing this section, we would like to mention that we used the numerical MF(2) data obtained for the reference system with $N = 25$ and for the $N \pm 1$ systems with 24 and 26 bosons to plot the diagrams presented in Figs.5. For all these systems we fixed the interaction strength at $\lambda_0 = 0.9/(25-1)$. The optimal occupations of the first and second orbitals at the minimum of the MF(2) energy curve of the reference system with 25 bosons are found to be $n_1^N = 23.08$ and $n_2^N = 1.92$, respectively. The non-integer occupation numbers appear due to the underlying mean-field approximation. They are to be considered as average values of the respective particle-number operators. We use these occupation numbers as the reference scale for the x-axes in Fig.5A and Fig.5B.

VII. BOSON TRANSFER ENERGIES AND THE ORIGIN OF THE MINIMA OF MF ENERGIES

We define the *boson transfer energy* (BTE) as the energy needed to transfer a boson from one orbital to the other. In the framework of the MF(2) theory we start with the system which has the energy ${}^N E(n_1, n_2)$ and evaluate the BTE as the energy difference between this energy and the energy of the "final" state where the occupation number of the first orbital is reduced by one to $n_1 - 1$ and the occupation number of the second orbital is increased by one to $n_2 + 1$. In principle, the energy needed to move a boson from the first orbital to the second one differs from the energy of the inverse process where a boson is transferred from the second orbital to the first one. The $BTE_{(1 \rightarrow 2)}$ and $BTE_{(1 \leftarrow 2)}$ are given by:

$$BTE_{(1 \rightleftharpoons 2)} = {}^N E(n_1 \mp 1, n_2 \pm 1) - {}^N E(n_1, n_2). \quad (21)$$

In the frozen orbital approximation the boson transfer energies can be straightforwardly evaluated using these definitions and the MF(2) expressions for the energies. The results take on the following form:

$$\begin{aligned} BTE_{(1 \rightarrow 2)} &= \mu_{22} - \mu_{11} + \frac{\lambda_0}{2} \int |\phi_2|^4 d\vec{r} - 2\lambda_0 \int |\phi_1|^2 |\phi_2|^2 d\vec{r} \\ BTE_{(1 \leftarrow 2)} &= \mu_{11} - \mu_{22} + \frac{\lambda_0}{2} \int |\phi_1|^4 d\vec{r} - 2\lambda_0 \int |\phi_1|^2 |\phi_2|^2 d\vec{r} \end{aligned} \quad (22)$$

These results will be used in the discussion below.

It is quite natural to suppose that at equilibrium an exchange of the particles between different orbitals (fragments) must be suppressed in the fragmented state. In other words, the energy needed to transfer a boson from the first orbital to the second one, is equal to the energy needed for the inverse process - a transition of the boson from the second orbital to the first one. Therefore, the difference between both boson transfer energies

$$Q = (BTE_{(1 \leftarrow 2)} - BTE_{(1 \rightarrow 2)})/2 \quad (23)$$

may serve as a criterion of how far we are from the equilibrium. Substituting the respective transition energies from Eqs.22 provides a senseful approximation for Q :

$$Q = \mu_{11} - \mu_{22} + \frac{\lambda_0}{2} \int |\phi_1|^4 d\vec{r} - \frac{\lambda_0}{2} \int |\phi_2|^4 d\vec{r} \quad (24)$$

To make contact with the MF(2) energy curves and to get deeper insight into the origin of the minima of these curves which determine the BMF(2) energy, it is worthwhile to consider the energy derivative $\frac{dE}{dn_1}$ with respect to the occupation number n_1 . To evaluate the derivative we use again the frozen orbital approximation which has been found to provide accurate results for the boson ionization potentials and affinities. In this approximation we can assume that the orbitals ϕ_i do not depend explicitly on the n_i and the direct differentiation of the energy in Eq.6 with respect to n_1 gives:

$$\frac{dE}{dn_1} = \mu_{11} - \mu_{22} + \frac{\lambda_0}{2} \int |\phi_1|^4 d\vec{r} - \frac{\lambda_0}{2} \int |\phi_2|^4 d\vec{r} \quad (25)$$

By comparing this derivative with the previous equation for Q one finds that they are identical.

At the optimal orbitals and occupation numbers the MF(2) energy takes on its minimum and $\frac{dE}{dn_1} = 0$ (see Figs.2 and 3). Consequently, our physical assumption that at the equilibrium the boson transfer energies are equal is fully supported by identifying Q with $\frac{dE}{dn_1}$. Moreover, if the bosonic system is not at equilibrium, then due to the difference between $BTE_{(1 \leftarrow 2)}$ and $BTE_{(1 \rightarrow 2)}$ a flow of bosons between the ϕ_1 -manifold and the ϕ_2 -manifold is enforced until equilibrium is reached. Therefore, the slope of the MF(2) energy curve given in Eq.25 can be viewed as the "driving force" for the flow of bosons between the two boson subsystems.

To verify these physically appealing results we investigate in more detail condensates with $N = 25$ and $N = 1000$ bosons at $\lambda = 0.9$. The lower panels of Fig.6 show values of Q for different values of n_1/N evaluated via Eq.24 using the frozen orbital approximation. Also shown is $\frac{dE}{dn_1}$ obtained by numerically differentiating the MF(2) energy curve in Fig.3 with respect to n_1/N for the same systems. On both pictures the values of the optimal occupation numbers n_1/N where the MF(2) energy curves take on their minima are marked by vertical dashed lines. From these figures it is clearly seen that indeed, at the minimum of the MF(2) energy, the flow of the particles between the fragments is completely suppressed, i.e., at the best mean-field state the driving force is equal to zero.

VIII. LARGE N LIMIT

In the large N limit, N as well as n_1 and n_2 are much larger than 1 and we may replace $N - 1$ by N . Repeating the calculations of the preceding sections one finds that all terms proportional to $\lambda_0 \times 1$ and not to $\lambda_0 \times N$ or $\lambda_0 \times n_i$, $i = 1, 2$, vanish in the large N limit. Accordingly, we find that in the large N limit not only the vertical boson ionization potentials are given by the chemical potentials as found in Sec.VI (see Eqs.14), but that also the vertical boson affinities are:

$$BA_V(k) = -\mu_{kk}, \quad k = 1, 2. \quad (26)$$

Obviously, also the boson affinity in the framework of the GP theory is determined by the corresponding GP chemical potential μ_{GP} in the large N limit.

In the large N limit the boson transfer energy $BTE_{(1 \rightarrow 2)}$ becomes identical to $-BTE_{(1 \leftarrow 2)}$. The energy needed to transfer a boson in a condensate with N particles from one fragment to the other one is just given by the difference of the corresponding potentials:

$$BTE_{(i \rightarrow j)} = \mu_{jj} - \mu_{ii} \quad (27)$$

This quantity is then nothing but $BIP_V(i) - BA_V(j)$ which is very appealing for large systems.

In the large N limit the quantity Q introduced in Eq.23 and the energy derivative with respect to the occupation number n_1 become identical and are just determined by the difference of the chemical potentials of the fragments. In particular, we find

$$\frac{dE}{dn_1} = \mu_{11} - \mu_{22} \quad (28)$$

which has been derived before in Ref.[14].

To illustrate the impact of the growing number of bosons in condensates we plot the diagonal Lagrange multipliers μ_{11} and μ_{22} as a function of the relative occupation number n_1/N for systems with $N = 25$ and $N = 1000$ bosons in the upper panels of Fig.6. In these panels the values of the optimal occupation numbers n_1/N obtained at the minima of the MF(2) energy curves $E(n_1)$ are marked by vertical dashed lines and the value of the chemical potential μ_{GP} obtained in the GP theory by a horizontal solid line.

One can see that for the systems with $N = 25$ bosons (see left upper panel of Fig.6) the crossing point of the $\mu_{11}(n_1/N)$ and $\mu_{22}(n_1/N)$ curves is located substantially aside from the

vertical dashed line. In contrast, the corresponding curves cross the vertical dashed line at almost the same value of n_1/N for the system with $N = 1000$ bosons (see right upper panel of Fig.6). However, on an enlarged scale as seen in the inset, the exact crossing point of the $\mu_{11}(n_1/N)$ and $\mu_{22}(n_1/N)$ curves lies aside from the vertical dashed line marking the value of the optimal occupation number n_1/N .

To better understand these results let us analyze Eq.25. The systems with $N = 25$ and $N = 1000$ bosons at $\lambda = 0.9$ are characterized by different values of $\lambda_0 = \lambda/(N - 1)$. Therefore, the contributions of the terms which are proportional to λ_0 in Eq.25 are much smaller for the system with $N = 1000$ than with $N = 25$ bosons where they play an important role. In other words, in the large N limit the flow of the bosons is determined by the differences of the chemical potentials $\mu_{11} - \mu_{22}$ only. Interestingly, $\frac{dE}{dn_1} = 0$ holds at the best mean field and consequently the chemical potentials of the fragments are identical to each other in the ground state of the condensate in the large N limit.

IX. CONCLUSIONS

In this article condensates with N identical repulsive bosons immersed into a double-well external potential have been investigated at different levels of multi-orbital mean-field theories where optimal orbitals and optimal occupation numbers are determined variationally.

At the level of one-orbital mean-field theory (Gross-Pitaevskii) the ground state of the system reveals a bifurcation scenario at a critical value of the non-linear parameter $\lambda_{cr} = \lambda_0(N - 1) = 0.837$. From this λ_{cr} on the delocalization of the bosons over the two wells of the trap potential becomes energetically more favorable than the localization of the BEC in the deeper well.

The two-orbital mean-field theory predicts the existence of two-fold fragmented states, i.e., both orbitals of these states are occupied macroscopically. Depending upon the number of particles in the BEC and/or the strength of the interparticle interaction, this fragmented state can be the ground state of the system. For condensates with a small number of particles the fragmented ground state is the only stable state, because the non-fragmented state predicted by the GP theory corresponds to the maximum of the energy in the two-orbital scenario.

By applying the three-orbital mean-field we verify numerically that for the double-well

external potential studied here the overall best mean field is achieved within two orbitals (BMF(2)). The inclusion of third orbital does not improve the mean-field description as the variational principle minimizes the energy at a vanishing population of the third orbital. Hence, the two-fold fragmented state obtained is the physical state of the system. Once $N \geq N_{max}$, where N_{max} depends on the interparticle interaction strength, the energy difference between the fragmented and the non-fragmented state may be very small, indicating that in these cases two physically different states may coexist.

Inspired by similarities between fragmented states in bosonic systems and shell structures in the fermionic world, we introduce vertical and adiabatic boson ionization potentials and boson affinities. In this respect we discuss the chemical potentials of the fragments and their relation to boson ionization and attachment measurements. The energy splitting between the values corresponding to the different fragments are small for systems with a large number of bosons while they might be distinguishable for systems with a small number of bosons.

We also introduced a boson transfer energy as the energy needed to move a boson from fragment "1" to fragment "2". We proved that only at equilibrium the same energy is needed for the inverse process where a boson is transferred from fragment "2" to fragment "1". It is argued that the difference between both boson transfer energies may serve as a criterion of how far we are from equilibrium. This difference is easily evaluated at each point of the multi-orbital energy surface and may speed up the search of the energy minimum.

Explicit expressions have been determined within the frozen orbital approximation for the boson ionization potentials, boson affinities and boson transfer energies. These expressions shed light on the physical content of the quantities. The frozen orbital approximation is based on the assumption that adding or removing a single boson from a system with N bosons will not strongly change the orbitals of the other bosons and hence these orbitals can be assumed unchanged. We present numerical results which demonstrate that this approximation is valid for the condensates studied here.

Finally, we would like to stress that the present findings are general and not at all restricted to the geometry of the double-well trap potential discussed here. We find similar results for other double- and multi-well trap potentials including potentials used in current experiments.

The authors acknowledge useful discussions with Ofir Alon and Kaspar Sakmann.

- [1] P. Nozieres and D. Saint James, J. Phys. (Paris) **43**, 1133 (1982). P. Nozieres, in Bose-Einstein Condensation, edited by A. Griffin, D.W. Snoke, and S. Stringari (Cambridge University Press, Cambridge, England, 1996).
- [2] C.J. Myatt, E.A. Burt, R.W. Ghrist, E.A. Cornell, and C.E. Wieman, Phys. Rev. Lett. **78**, 586 (1997).
- [3] D.S. Hall, M.R. Matthews, J.R. Ensher, C.E. Wieman, and E.A. Cornell, Phys. Rev. Lett. **81**, 1539 (1997).
- [4] B.D. Esry and C.H. Greene, Phys. Rev. A **59**, 1457 (1998).
- [5] C.K. Law, H. Pu, N.P. Bigelow, and J.H. Eberly, Phys. Rev. Lett. **79**, 3105 (1997).
- [6] T.L. Ho and V.B. Shenoy, Phys. Rev. Lett. **77**, 3276 (1996).
- [7] M.A. Cazalilla and A.F. Ho, Phys. Rev. Lett. **91**, 150403 (2003).
- [8] A.A. Svidzinsky and S.T. Chui, Phys. Rev. A **67**, 053608 (1998).
- [9] E.P. Gross, Nuovo Cimento **20**, 454 (1961).
- [10] L.P. Pitaevskii, Sov. Phys. JETP **13**, 451 (1961).
- [11] A.S. Parkins and D.F. Walls, Phys. Rep. **303**, 1 (1998).
- [12] F. Dalfovo, S. Giorgini, L.P. Pitaevskii, and S. Stringari, Rev. Mod. Phys. **71**, 463 (1999).
- [13] L.S. Cederbaum and A.I. Streltsov, Phys. Lett. A **318**, 564 (2003).
- [14] L.S. Cederbaum and A.I. Streltsov, Phys. Rev. A **70**, 023610 (2004).
- [15] A.I. Streltsov and L.S. Cederbaum, N. Moiseyev, Phys. Rev. A **70** 053607 (2004).
- [16] M. Albiez, R. Gati, J. Foelling, S. Hunsmann, M. Cristiani, and M.K. Oberthaler, e-print cond-mat/0411757.
- [17] C. Huepe, S. Métens, G. Dewel, P. Borckmans, and M.E. Brachet, Phys. Rev. Lett. **82**, 1616 (1999).
- [18] P. Couillet and N. Vandenberghe, Phys. Rev. A **64**, 025202(R) (2001).
- [19] S. Komineas and N. Papanicolaou, Phys. Rev. A **68**, 043617 (2003).
- [20] R. D'Agosta and C. Presilla, Phys. Rev. A **65**, 043609 (2003).
- [21] M. Holthaus, Phys. Rev. A **64**, 011601(R) (2001); M. Holthaus and S. Stenholm, Eur. Phys. J. B **20**, 451 (2001).

- [22] O.E. Alon, A.I. Streltsov, K. Sakmann, and L.S. Cederbaum, *Europhys. Lett.* **67**, 8 (2004).
- [23] O. Penrose and L. Onsager, *Phys. Rev.* **104**, 576 (1956).
- [24] J. Javanainen and S.M. Yoo, *Phys. Rev. Lett.* **76**, 161 (1996).
- [25] Y. Castin, J. Dalibard, *Phys. Rev. A* **55**, 4330 (1997).
- [26] J. Javanainen and M.Yu. Ivanov, *Phys. Rev. A* **60**, 2351 (1999).
- [27] J. Ruostekoski and D.F. Walls, *Phys. Rev. A* **58**, R50 (1998).
- [28] F. Meier and W. Zwerger, *Phys. Rev. A* **64**, 033610 (2001).
- [29] S. Raghavan, A. Smerzi, S. Fantoni and S.R. Shenoy, *Phys. Rev. A* **59**, 620 (1999).
- [30] L. Pitaevskii and S. Stringari, *Phys. Rev. Lett.* **87**, 180402 (2001).
- [31] A. Szabo and N.S. Ostlund, *Modern Quantum Chemistry*, Dover, Mineola, NY (1996).
- [32] T. Koopmans, *Physica*, **1**, 104 (1933).

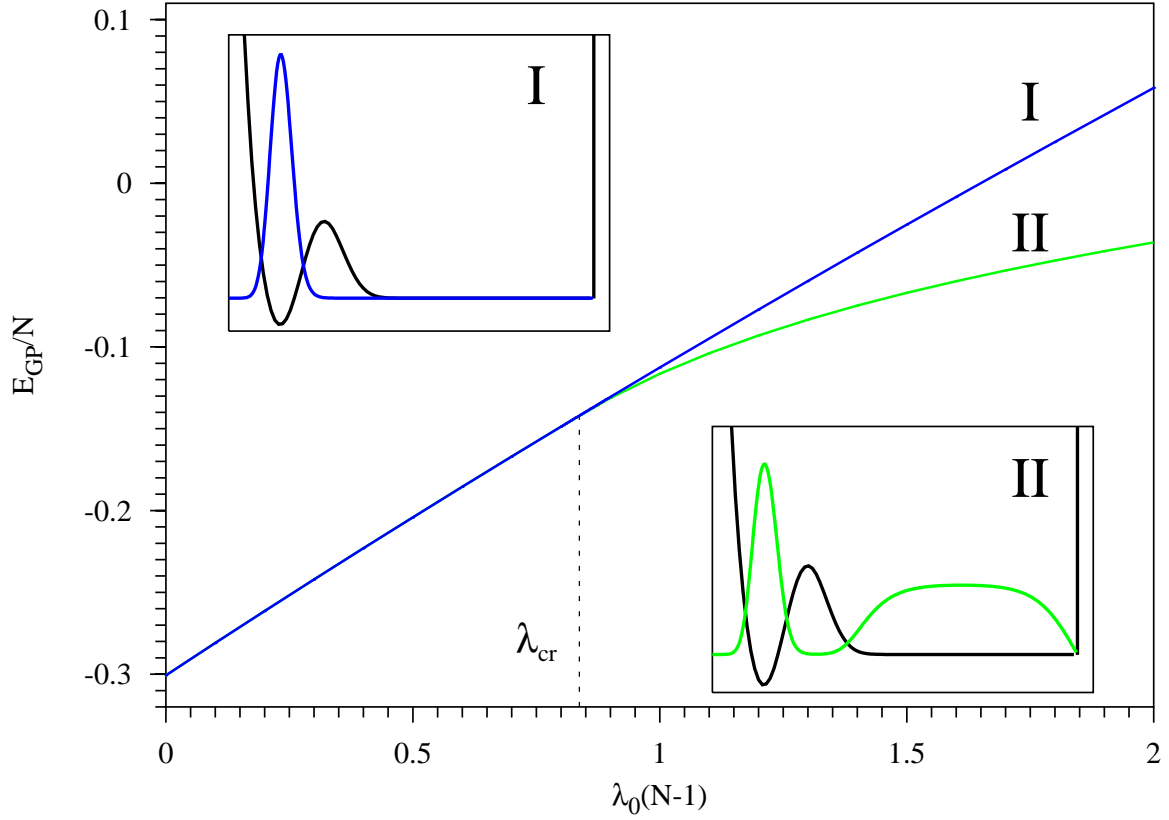


FIG. 1: (Color online) Results of one-orbital mean-field (GP) theory. Shown are the energies per particle E_{GP}/N of the lowest energy solutions of the Gross-Pitaevskii equation as a function of $\lambda = \lambda_0(N-1)$. The bifurcation point observed at $\lambda_{cr} = 0.837$ is marked by a dash line. In the insets the GP orbitals corresponding to the upper (I) and lower (II) energy branches are depicted together with the double-well trap potential. The values of the external trap potential (for parameters, see text) have been scaled by $1/10$. All energies are given in units of ω . All orbitals are dimensionless and plotted as functions of the dimensionless coordinate x .

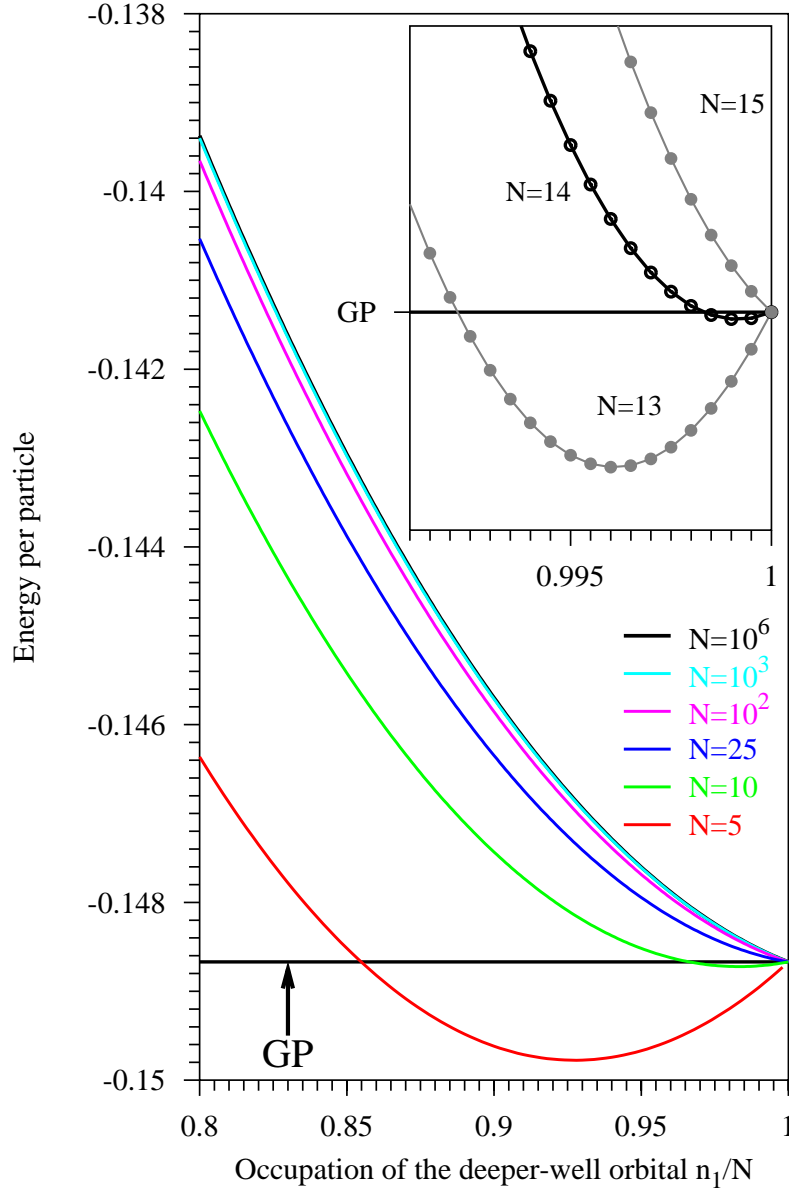


FIG. 2: (Color online) Results of the two-orbital mean-field (MF(2)) theory for $\lambda = 0.8 < \lambda_{cr}$. Shown are energies per particle for condensates made of $N = 5, 10, 25, 10^2, 10^3$ and 10^6 bosons as a function of the relative occupation number n_1/N of the orbital localized in the deeper well. The horizontal solid line labeled as "GP" shows the corresponding GP energy per particle. In the inset the energy per particle for the systems with $N = 13, 14$ and 15 bosons are plotted. All energies are given in units of ω .

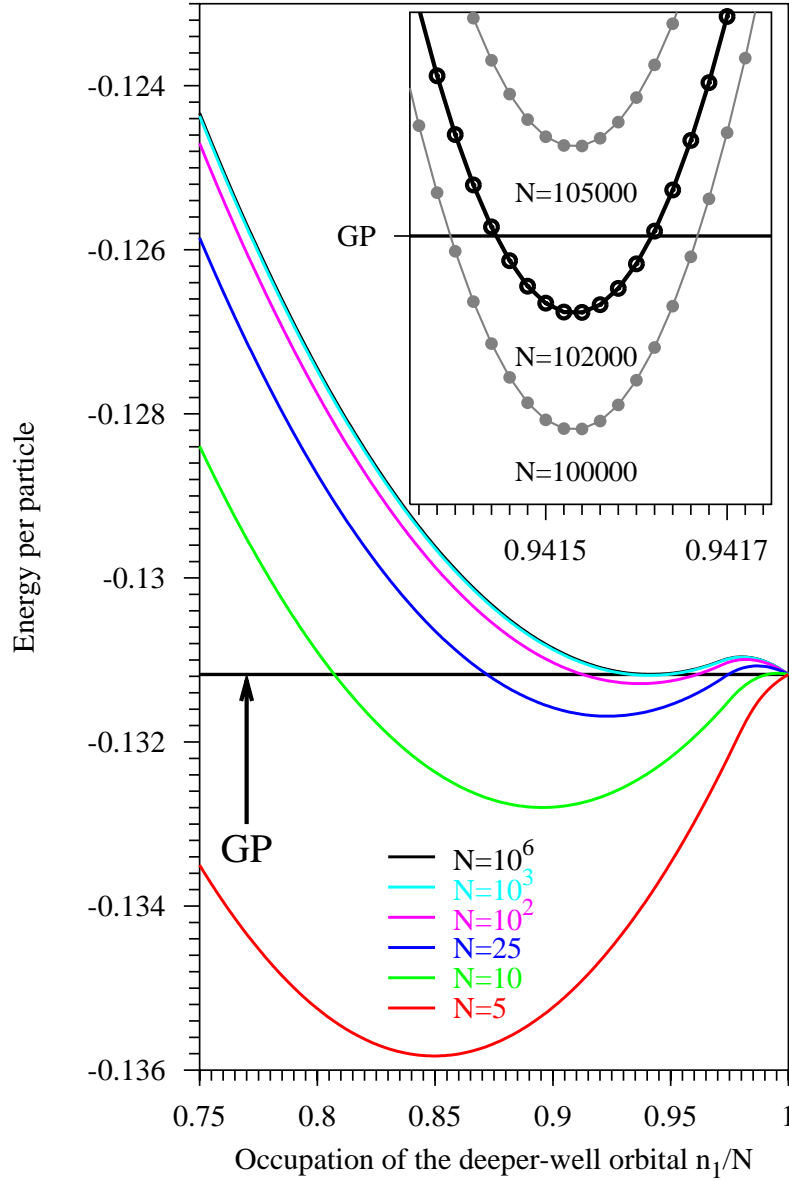


FIG. 3: (Color online) Results of the two-orbital mean-field (MF(2)) theory for $\lambda = 0.9 > \lambda_{cr}$. Shown are energies per particle for condensates made of $N = 5, 10, 25, 10^2, 10^3$ and 10^6 bosons as a function of the relative occupation number n_1/N of the orbital localized in the deeper well. The horizontal solid line labeled as "GP" shows the corresponding GP energy per particle. In the inset the energy per particle for the systems with $N = 100000, 102000$ and 105000 bosons are plotted. All energies are given in units of ω .

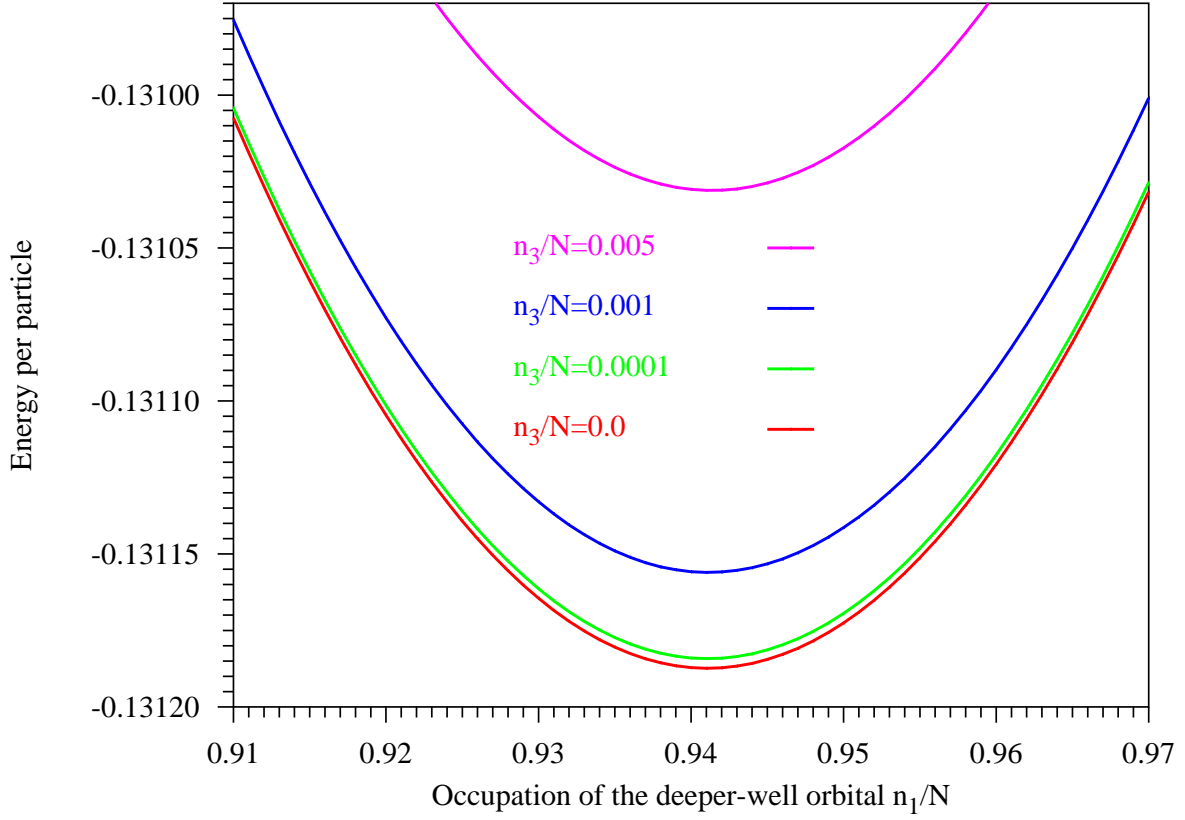


FIG. 4: (Color online) Demonstration that BMF(2) provides the overall best mean field. Shown are the results obtained with the three-orbital mean-field (MF(3)) theory for $N = 1000$ bosons and $\lambda = \lambda_0(N - 1) = 0.9$. Plotted are the energy per particle as a function of the relative occupation number n_1/N for fixed values of the third relative occupation number n_3/N . The curves shown correspond to $n_3/N = 0.0, 0.0001, 0.001$ and 0.005 . All energies are given in units of ω .

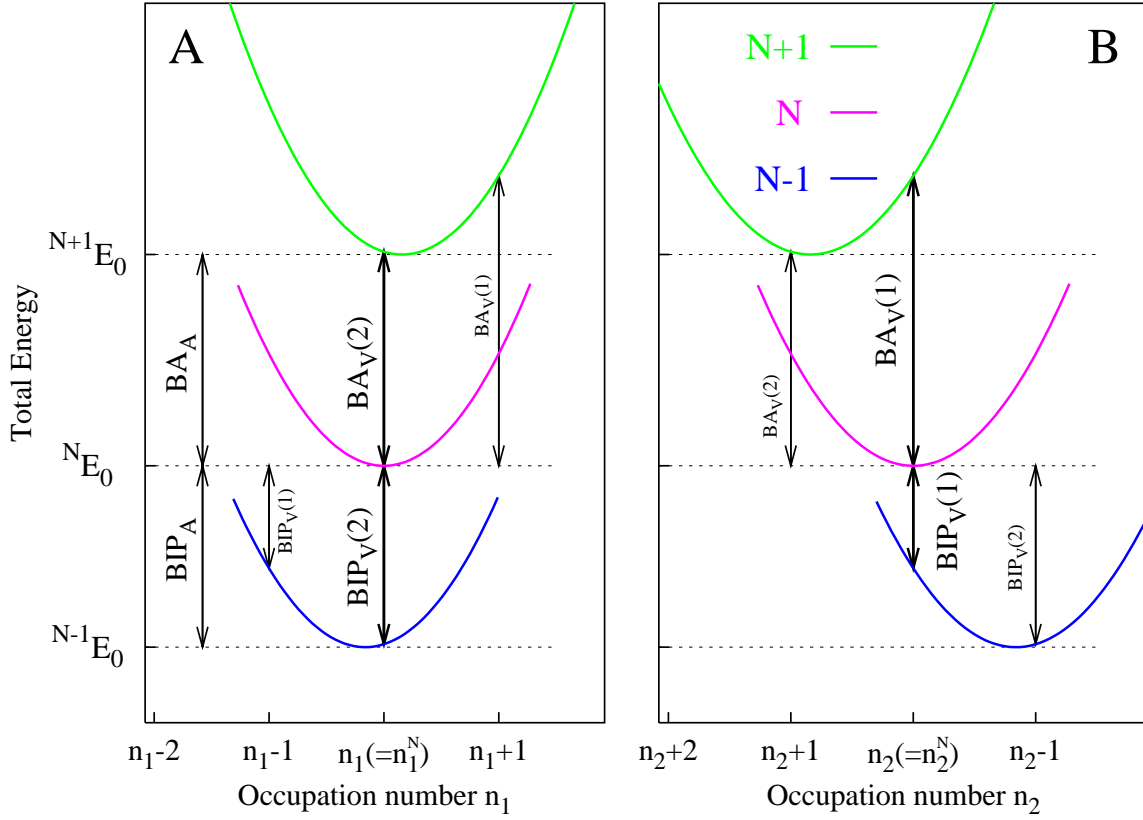


FIG. 5: (Color online) Schematic diagram defining the boson ionization potentials (BIP) and boson affinities (BA). Total energies of condensates with $N - 1$, N and $N + 1$ bosons obtained within the framework of the MF(2) theory are plotted in the left figure (A) as a function of the occupation number n_1 and in the right figure (B) as a function of the occupation number $n_2 = N - n_1$. The minima of the energy curves are denoted by $^{N-1}E_0$, NE_0 and $^{N+1}E_0$, and are indicated on the energy axis. The reference condensate for which the boson ionization potentials and boson affinities are defined is that with N particles. The optimal occupation numbers of this condensate are n_1^N and n_2^N . Vertical and adiabatic boson ionization potentials and boson affinities are shown (see text for more details).

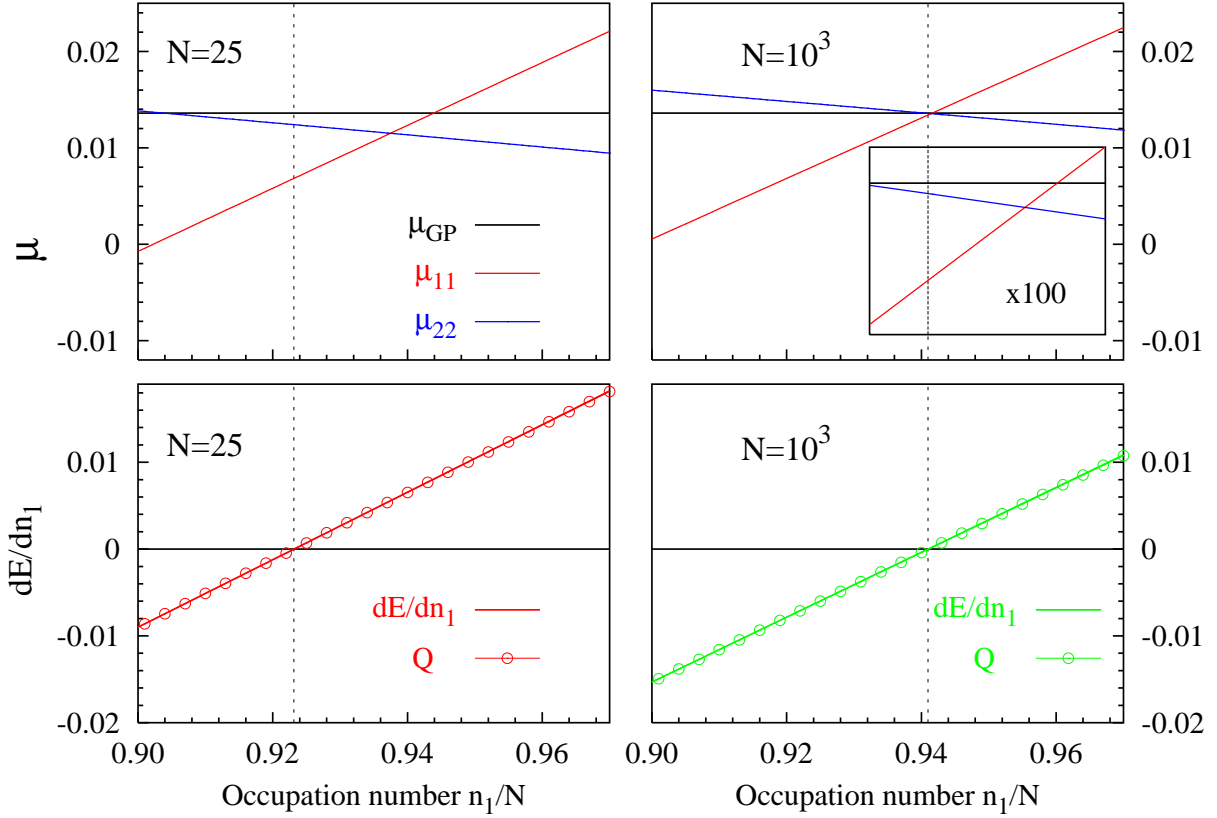


FIG. 6: (Color online) The upper two panels show the chemical potentials (diagonal Lagrange multipliers) μ_{11} and μ_{22} for condensates with $N = 25$ and $N = 1000$ bosons as a function of the relative occupation number n_1/N . For comparison, the horizontal solid line shows the value of the corresponding chemical potential μ_{GP} obtained in the GP theory. The inset shows the same curves on a much ($\times 10^2$) enlarged scale. The lower two panels depict the derivative dE/dn_1 (solid line) of the total energy with respect to n_1 and the difference between the boson transfer energies Q (points) for the same systems as in the upper panels. dE/dn_1 is obtained by numerical differentiation of the MF(2) energy curves and Q is evaluated using Eq.24. The vertical dashed lines mark the values of the optimal occupation numbers n_1/N obtained at the minima of the corresponding energy curves. $\lambda = 0.9$ is used throughout. The energy derivatives and all chemical potentials are given in units of ω .

TABLE I: The adiabatic and vertical boson ionization potentials BIP_A and $BIP_V(k)$ and boson affinities BA_A and $BA_V(k)$ for condensates with $N = 5, 10, 25, 100$ and 1000 bosons. Shown are quantities evaluated according to their definitions in Eqs.11,12 and 16,17 as differences of total energies and compared with those computed using the frozen orbital approximation in Eqs.14 and 19. These approximate numbers are given in parenthesis. $\lambda = 0.9$ is used throughout.

N	Ionization			Affinity		
	BIP_A	$BIP_V(1)$	$BIP_V(2)$	BA_A	$BA_V(1)$	$BA_V(2)$
5	-0.007508	0.025694	-0.006132	-0.020167	-0.052911	-0.021267
		(0.027242)	(-0.006248)		(-0.055309)	(-0.021819)
10	-0.010946	0.003733	-0.010390	-0.016514	-0.031100	-0.017021
		(0.004460)	(-0.010387)		(-0.031993)	(-0.017142)
25	-0.012613	-0.007123	-0.012412	-0.014692	-0.020167	-0.014886
		(-0.006844)	(-0.012405)		(-0.020470)	(-0.014910)
100	-0.013361	-0.012032	-0.013314	-0.013865	-0.015193	-0.013912
		(-0.011964)	(-0.013311)		(-0.015262)	(-0.013916)
1000	-0.013576	-0.013445	-0.013572	-0.013626	-0.013758	-0.013631
		(-0.013438)	(-0.013571)		(-0.013764)	(-0.013631)
$\mu_{GP} = 0.013599$						